

Figure S1

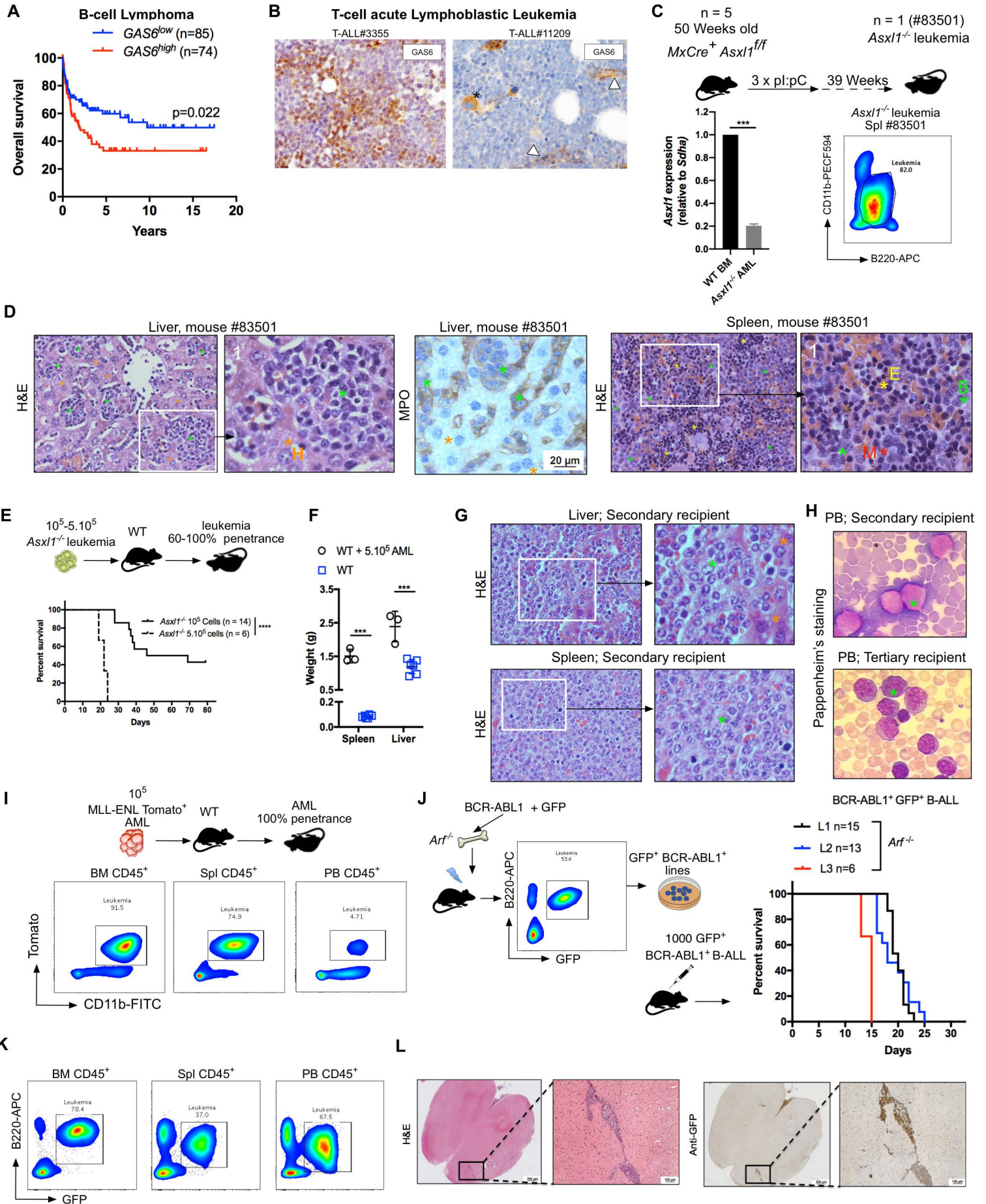


Figure S1. Significance of GAS6 expression in hematological cancers and pre-clinical models used in this study.

(A) Prognostic value of *GAS6* expression in B-cell lymphoma (GSE4475 dataset, n=159). Data generated using the KaplanScan mode from the R2 Genomics Analysis and Visualization Platform (<http://r2.amc.nl>). Survival analysis by log-rank (Mantel–Cox) test.

(B) *GAS6* expression by IHC on bone marrow trephine biopsies from T-ALL patients at diagnosis. Asterisk marks a megakaryocyte. Stromal cells marked by white pyramid.

(C) Schematic view of the generation of an acute leukemia model driven by *Asx1* loss in hematopoietic cells (detailed description provided in Supplementary Methods). 39 weeks post *Asx1* ablation, one primary mouse (1/5, #83501) developed a disease characterized by the expansion of cells with significantly reduced *Asx1* expression as shown by real time PCR and an aberrant CD11b^{dim}B220^{dim} immature surface phenotype. Real-time PCR data are means \pm s.e.m. after normalization to a reference gene, *Sdha*.

(D) H&E staining on liver and spleen, as well as myeloperoxidase staining (MPO) on liver sections from mouse #83501 described in C. Green asterisk: Myeloid blasts; Yellow asterisk: Erythroid lineage cells; Red asterisk: Megakaryocyte; Orange asterisk: Hepatocyte.

(E) Spleen cells from the leukemic mouse described in C, were transferred to secondary and tertiary C57BL/6 recipients without prior conditioning. In secondary recipients, 100% disease penetrance was observed when $5 \cdot 10^5$ primary cells are injected (n = 5), and 60-80% if 10^5 cells are injected (n = 14).

(F) Disease-bearing secondary recipients show hepatosplenomegaly (n = 5 WT controls; n = 3 WT mice challenged with *Asx1*^{-/-} cells from (C)). ***p<0.001, unpaired two-tailed Student's *t*-test.

(G) H&E staining on spleen and liver sections from a secondary recipient mouse. Green asterisk: Myeloid blasts; Orange asterisk: Hepatocyte.

(H) Pappenheim staining of peripheral blood smears from both secondary and tertiary recipient mice, demonstrating the presence of myeloblasts with fine cytoplasmic granules.

(I) Injection of 10^5 MLL-ENL tomato⁺ leukemia cells to non-conditioned C57BL/6 mice propagates leukemia in 100% of the animals as depicted by flow cytometry data showing CD11b⁺ tomato⁺ leukemic infiltrate in the bone marrow and spleen of diseased animals. Leukemic blasts are also detected in the peripheral blood albeit at a lower frequency.

(J) Schematic description of the generation of primary GFP⁺ BCR-ABL1⁺ B-ALL leukemia in an *Arf*^{-/-} background (detailed description provided in Supplementary Methods). After a short adaptation period on MS5 mesenchymal stromal cells, primary leukemic cells could be expanded and maintained as primary GFP⁺ leukemic lines in a stroma-independent fashion. Kaplan-Meier survival analysis of non-irradiated secondary recipient mice transplanted with a 10^3 GFP⁺ B-ALL cells from n = 3 independent primary leukemia lines (L1, L2 and L3). Disease penetrance and latency were comparable for all 3 leukemias.

(K) Mice from (I) exhibit full-blown leukemia that can be detected as GFP⁺ B220⁺ blasts by FACS in the bone marrow, spleen and peripheral blood.

(L) H&E and anti-GFP IHC analysis show the presence of GFP⁺ leukemic blasts in the brain of leukemic mice.

Figure S2

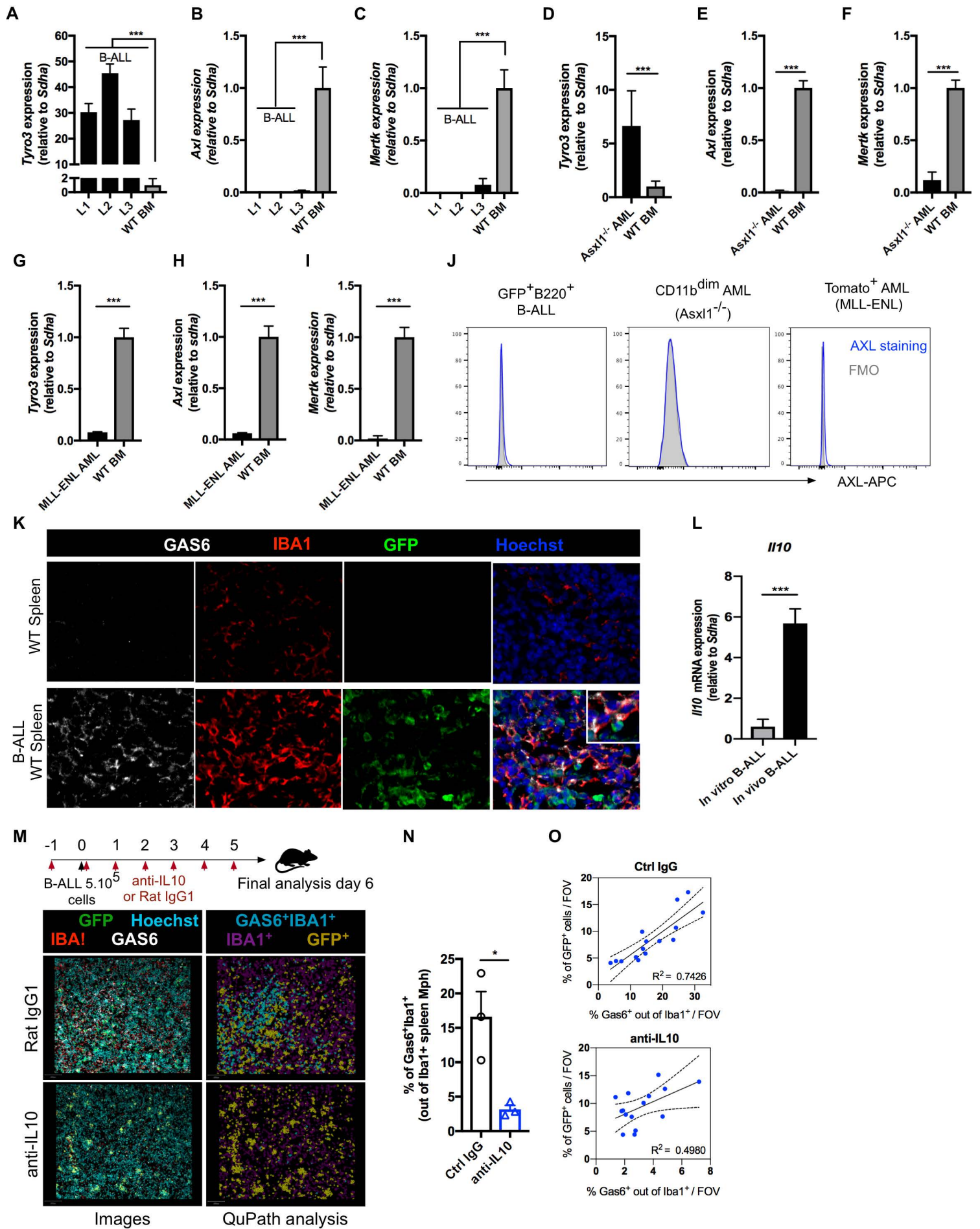


Figure S2. Expression pattern of TAM RTKs in murine leukemic cells and GAS6 induction in leukemia associated macrophages.

(A-I) TAM (*Tyro3*, *Axl* and *Mertk*) RTKs expression as evaluated by real-time PCR in L1, L2, and L3 B-ALL (GFP⁺ B220⁺) **(A-C)** as well as FACS purified *Asx1*^{-/-} AML cells (CD11b^{dim}B220^{dim}) **(D-F)** or *MLL-ENL* AML (Tomato⁺ CD11b⁺) **(G-I)**. In (A-I) WT bone marrow cells were used as a reference (WT BM) and all data are mean ± s.e.m. after normalization to a reference gene, *Sdha*. ***p<0.001, unpaired two-tailed Student's *t*-test.

(J) *Axl* expression as evaluated by flow cytometry in CD45⁺ leukemic blasts from mice with B-ALL (GFP⁺B220⁺), *Asx1*^{-/-} AML (CD11b^{dim}) or *MLL-ENL* AML (Tomato⁺ CD11b⁺). Full stain minus one (FMO for *Axl*) was used as negative reference.

(K) Representative immune-fluorescence images assessing the expression of Gas6 (white) in *Iba1*⁺ macrophages (red) from WT and B-ALL-bearing (GFP) mice.

(L) *Il10* expression as evaluated by real-time PCR in B-ALL cells (B220⁺GFP⁺) expanded *ex-vivo* (n = 4) or FACS purified from leukemia bearing mice (n = 6). Data are mean ± s.e.m. after normalization to a reference gene, *Sdha*. ***p<0.001, unpaired two-tailed Student's *t*-test.

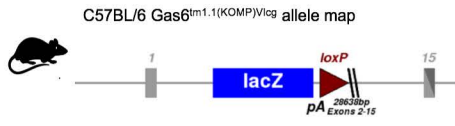
(M) Representative immune fluorescence staining with corresponding phenotypic segmentation using QuPath version 0.2.3, depicting Gas6 expression in *Iba1*⁺ macrophages in the spleen of mice that were challenged with B-ALL and treated with either an anti-IL10 (n = 3) or a Rat IgG1 (n = 3) control antibody (300 µg/mouse/day).

(N) Depicts the percentage of macrophages that express Gas6 in spleen samples from M. Each data point represents a mean of 5 field of views (FOV) from one independent mouse. *p<0.05, unpaired two-tailed Student's *t*-test.

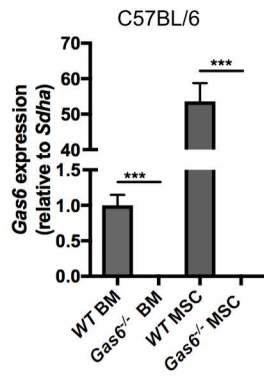
(O) Correlation analysis between the percentage of leukemic blasts per field of view (% GFP⁺ cells/ FOV) and the percentage of Gas6-expressing macrophages per field of view (% Gas6⁺ out of *Iba1*⁺/ FOV) in the spleen of mice from M. each dot represents an independent FOV. Five FOVs were analyzed for each mouse.

Figure S3

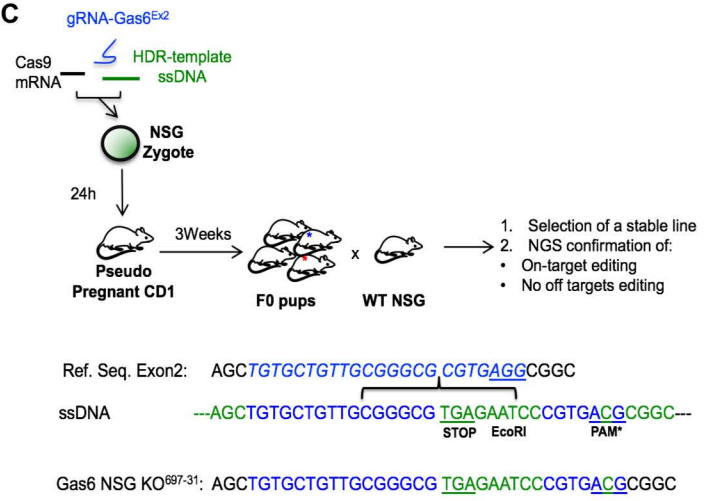
A



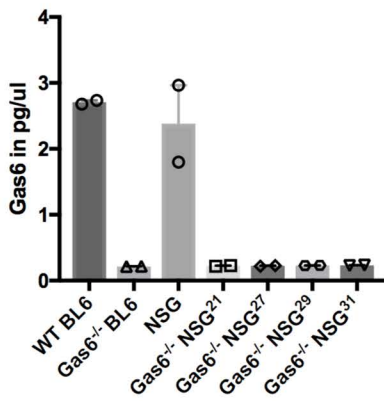
B



C



D



E

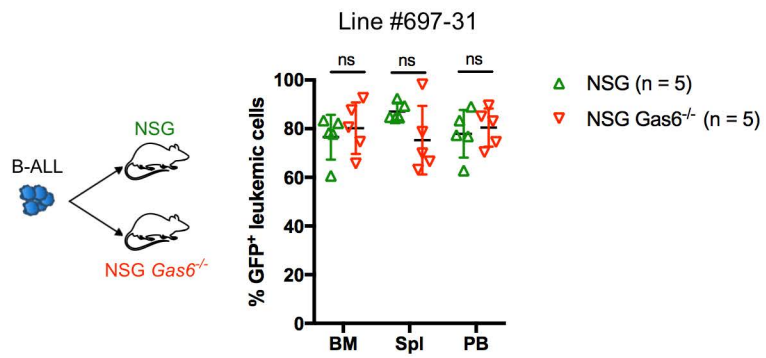


Figure S3. Generation and characterization of *Gas6*-deficient mouse lines in a C57BL/6 immune-competent and *NOD.Cg-Prkdc^{scid} IL2rgtmWjl/Sz* (NSG) immune-compromised background.

A, C57BL/6 *Gas6* knock out mice were obtained from the Knock Out Mouse Project (KOMP) Repository (<https://www.komp.org/index.php>). A schematic view of the knockout allele is indicated.

B, *Gas6* expression as evaluated by real-time PCR, both in hematopoietic bone marrow cells (BM) and mesenchymal stromal cells (MSC). *** $p < 0.001$, unpaired two-tailed Student's *t*-test.

C, Immune-compromised *Gas6*-deficient mice were generated by inactivation of the *Gas6* gene using CRISPR-Cas9 editing in *NOD.Cg-Prkdc^{scid} IL2rgtmWjl/Sz* (NSG) zygotes following a workflow that was previously described by our group (Tirado-Gonzalez et al., 2018). This workflow relies on the use of a donor DNA template and homology directed repair (NSG lack functional non-homologous end-joining repair mechanism). The donor DNA template introduces a stop codon in exon 2 of the *Gas6* gene (to promote non-sense mediated mRNA decay), an EcoR-I site for screening purposes and a silent mutation in the PAM sequence to avoid secondary editing of any productively edited allele. Four independent NSG *Gas6*-deficient lines were generated (697-21, 27, 29 and 31).

D, *Gas6* protein was undetectable both in C57BL/6 *Gas6*^{-/-} and all four NSG *Gas6*^{-/-} lines as shown by ELISA (n = 2 mice per genotype).

E, Validation of data obtained in Fig. 1N, using a different NSG *Gas6*^{-/-} line and demonstrating comparable leukemic burden in WT versus *Gas6*^{-/-} NSG challenged with B-ALL (NSG n = 5, NSG^{#697-31} *Gas6*^{-/-} n = 5).

Figure S4

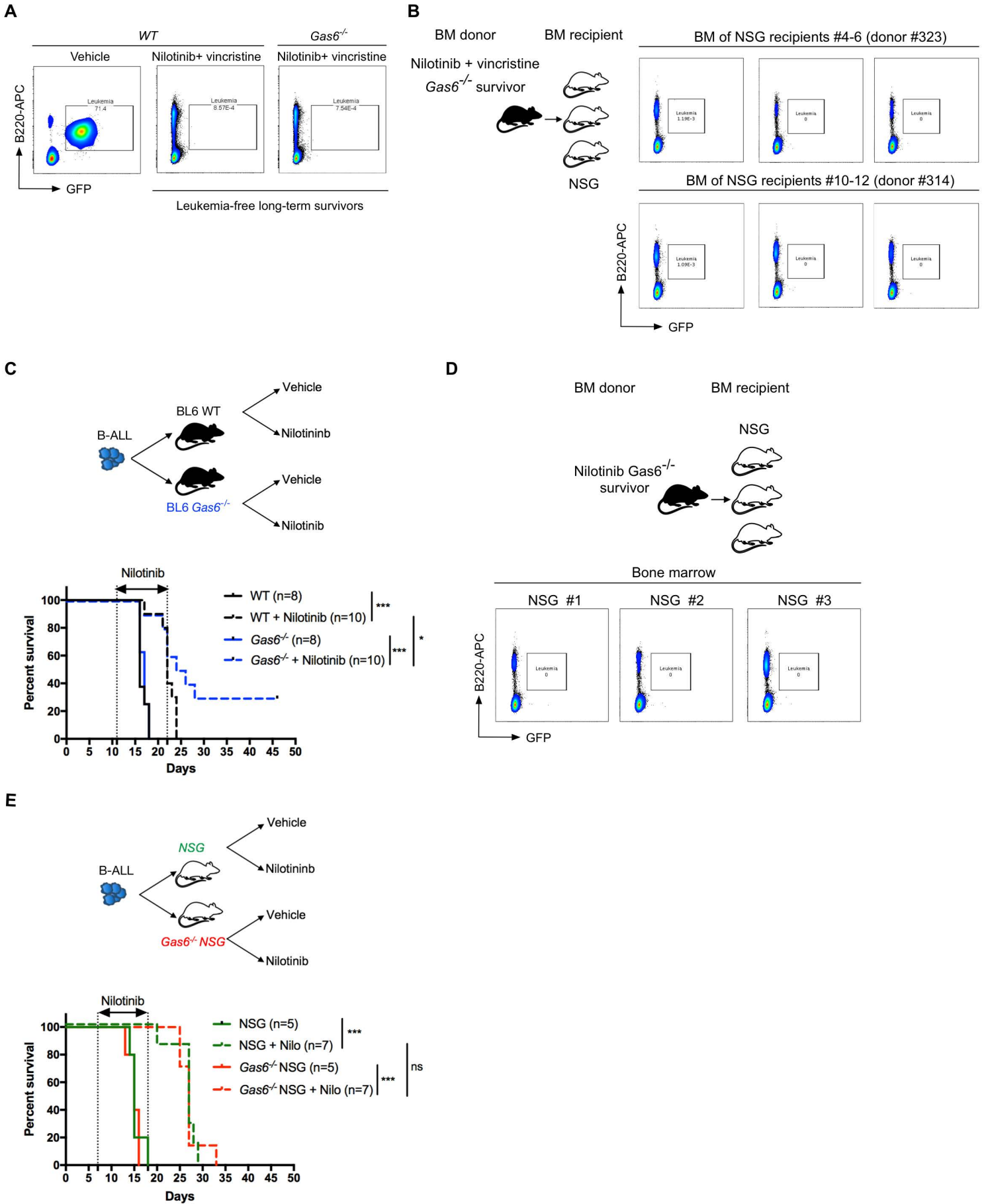


Figure S4. *Gas6* deficiency in the environment synergizes with standard of care treatment to potentiate Ph⁺ B-ALL clearance.

(A) representative FACS data depicting the leukemic burden (B220⁺ GFP⁺) in the bone marrow of mice from Fig. 1Q.

(B) representative FACS data depicting lack of leukemia cells in the bone marrow of NSG mice 30 days after receiving 5.10⁶ bone marrow cells isolated from nilotinib and vincristine-treated *Gas6*^{-/-} long-term survivors displayed in Fig. 1Q. In total BM cells from n = 2 donors were each transferred to n = 3 NSG recipients (total n = 6 NSG recipients), none of which developed leukemia.

(C) Kaplan–Meier survival analysis of C57BL/6 WT and *Gas6*^{-/-} mice challenged with Ph⁺ B-ALL cells (10³) and treated with either vehicle or nilotinib. *p<0.05, ***p<0.001, log-rank (Mantel–Cox) test.

(D) FACS data depicting lack of leukemia cells in the bone marrow of NSG mice 30 days after receiving 5.10⁶ bone marrow cells isolated from a nilotinib-treated *Gas6*^{-/-} long-term survivor from C. BM cells from one donor were transferred to n = 3 NSG recipients.

(E) same as C, using immune compromised NSG mice. ns, not significant, ***p<0.001, log-rank (Mantel–Cox) test.

In C and E, treatments were initiated and stopped on the days indicated by dotted lines.

Figure S5

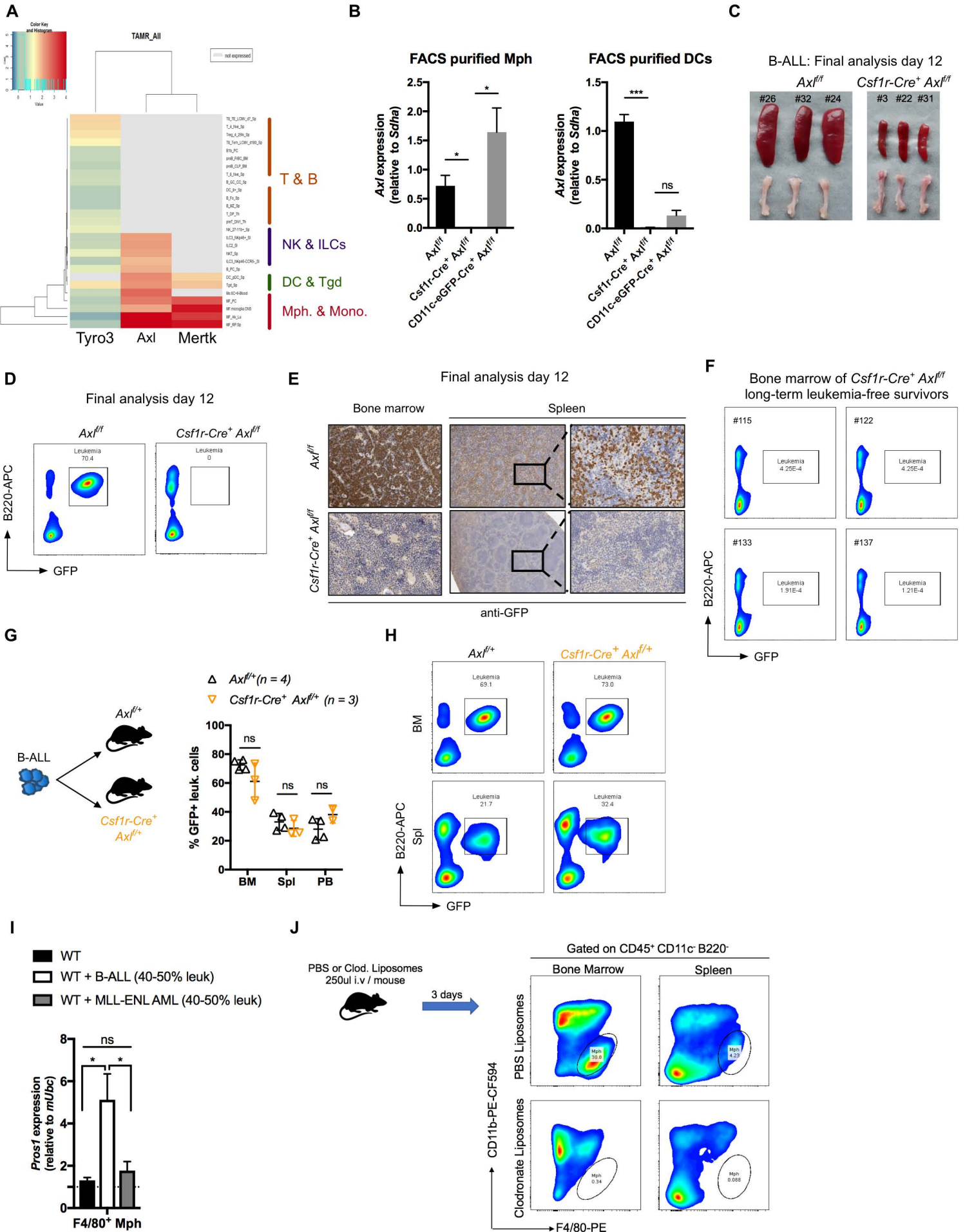


Figure S5. *Axl* deletion in macrophages triggers a potent anti-leukemic immune response against acute leukemia.

(A) Heat map of publicly available data from the immunological genome project depicting the expression levels of *Tyro3*, *Axl* and *Mertk* in different immune subsets, in mice. *Axl* displays highest expression in red pulp macrophages (MF_RP.Sp), lung alveolar macrophages (MF_Alv_Lu) and Ly6C⁺ blood monocytes (Mo.6C+II-Blood).

(B) *Axl* expression by real-time PCR in FACS purified macrophages (Mph: CD45⁺CD11c⁻F4/80⁺CD11b^{low}) and dendritic cells (DCs: CD45⁺CD11c⁺MHC-II⁺) isolated from the spleens of *Axl^{fl/fl}* (n = 3), *Csf1r-cre⁺ Axl^{fl/fl}* (n = 3) and *CD11c-eGFP-Cre Axl^{fl/fl}* (n = 6) mice. Purity of the sorted cells was over 95%. Data are mean ± s.e.m. after normalization to a reference gene, *Sdha*. ns, not significant, *p<0.05, ***p<0.001, unpaired two-tailed Student's *t*-test.

(C-E) Representative pictures of spleens and femurs (C), FACS data (D) and GFP IHC staining (E) depicting the B-ALL leukemic burden (on day 12) in the organs of mice of the indicated genotypes from Figure 2B.

(F) Representative FACS data showing no detectable leukemia cells in the bone marrow of four independent *Csf1r-Cre⁺ Axl^{fl/fl}* long-term survivors (#115, #122, #133, #137) initially challenged with B-ALL and depicted in Figure 2C.

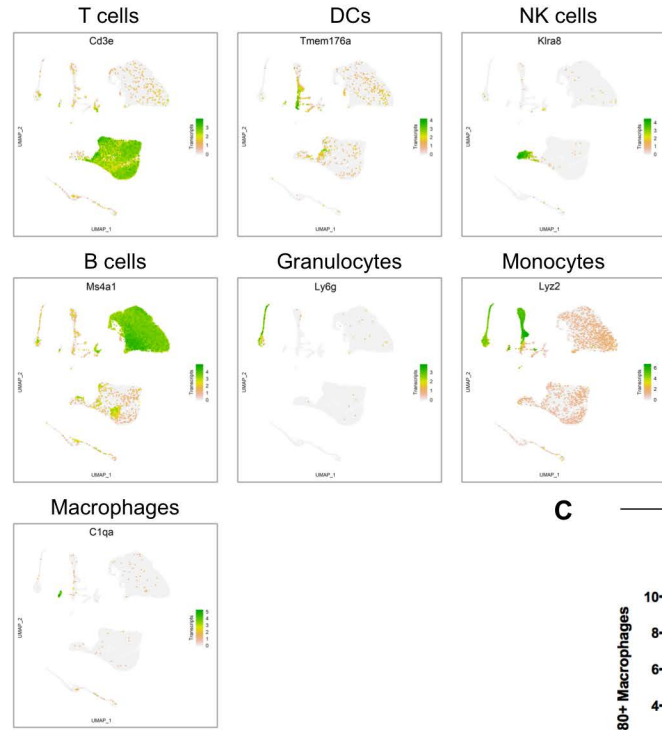
(G-H) Leukemic burden (G) in the bone marrow (BM), spleen (Spl) and peripheral blood (PB) as well as representative flow-cytometry plots depicting the percentage of leukemic cells (B220⁺ GFP⁺) in Control (*Axl^{fl/fl}*, n = 4) and *Csf1r-Cre*-expressing *Axl^{fl/fl}* mice (*Csf1r-Cre⁺ Axl^{fl/fl}*, n = 3) 12 days after challenged with 10³ B-ALL cells. ns, not significant, unpaired two-tailed Student's *t*-test.

(I) *Pros1* expression as evaluated by real-time PCR in MACS purified F4/80⁺ macrophages from wild type mice (n = 4) and mice challenged with B-ALL (n = 4) or MLL-ENL AML (n = 4). *p<0.05, unpaired two-tailed Student's *t*-test.

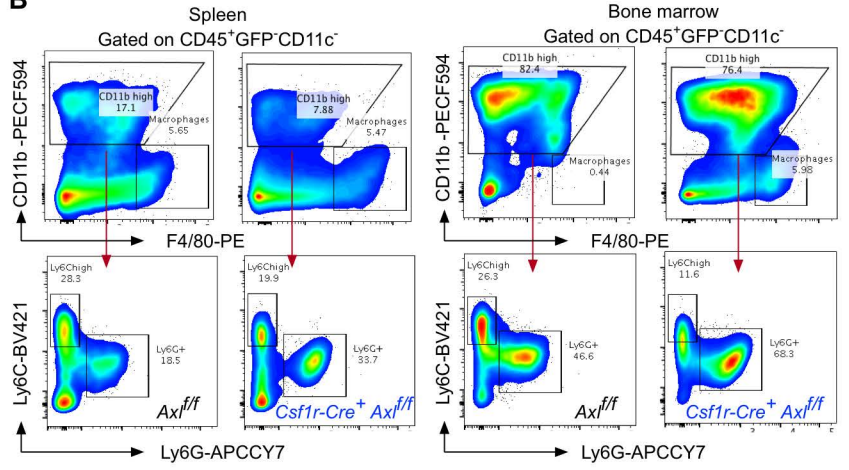
(J) Representative FACS data depicting the frequency of macrophages defined as CD45⁺CD11c⁻B220⁻CD11b^{low}F4/80⁺, in the spleen and bone marrow of mice treated with 250 µl of either PBS-loaded or clodronate-loaded liposomes. Liposomes were administered intravenously and mice analyzed 3 days post-injection.

Figure S6

A

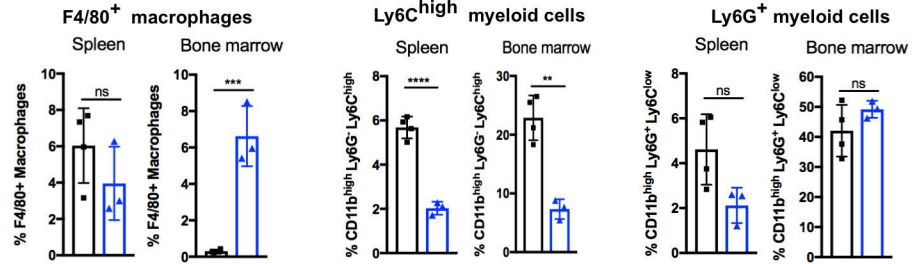


B

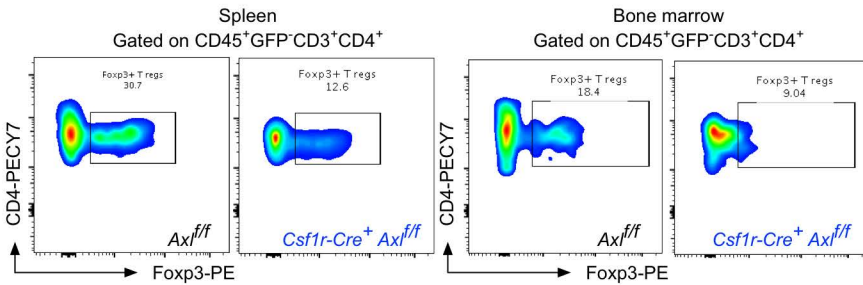


Frequencies out of non-leukemic CD45⁺ cells

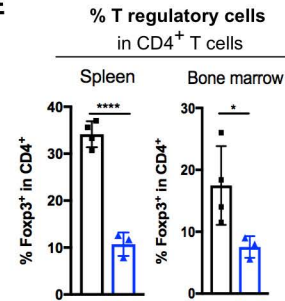
C



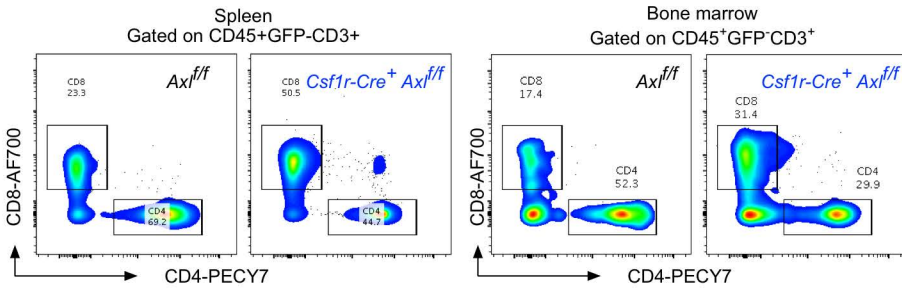
D



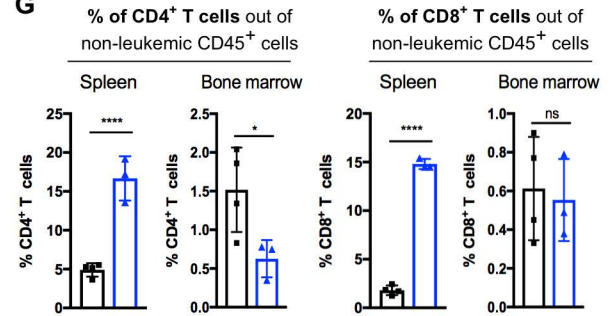
E



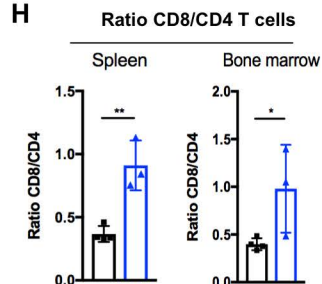
F



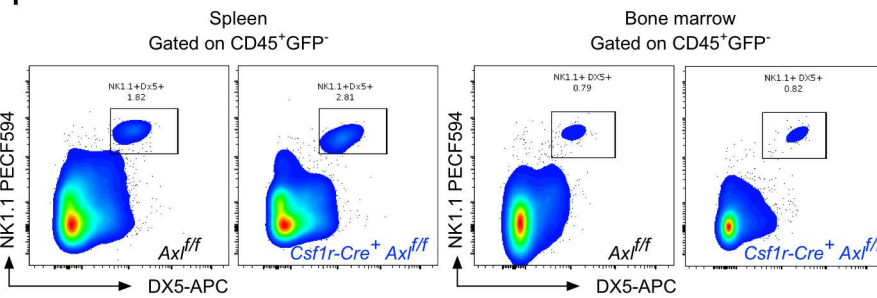
G



H



I



J

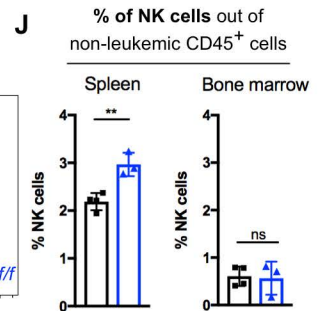


Figure S6. *Axl* ablation protects leukemia challenged mice from acquiring an immune suppressive microenvironment.

(A) Expression of *Cd3e* (T cells), *Tmem176a* (DCs), *Klra8* (NK cells), *Ms4a1* (B cells), *Ly6G* (Granulocytes), *Lyz2* (Monocytes) and *C1qa* (Macrophages) overlaid on the UMAP representation.

(B-C) Gating strategy and frequencies of myeloid subsets in the non-leukemic GFP⁻CD45⁺ fraction of cells from the bone marrow and spleen of *Axl^{fl/fl}* (n = 4) and *Csf1r-Cre⁺ Axl^{fl/fl}* (n = 3) animals analyzed on day 11 post-challenge with 10³ B-ALL cells. *Csf1r-Cre⁺ Axl^{fl/fl}* had no detectable leukemia, while *Axl^{fl/fl}* exhibited a mean leukemic burden of 51% in the bone marrow and 30% in spleen (data not shown). Macrophages: CD11c⁻CD11b^{low}F4/80^{high}; Ly6C^{high} Myeloid cells: CD11c⁻CD11b^{high} Ly6G⁻Ly6C^{high}; Ly6G⁺ Myeloid cells: CD11c⁻CD11b^{high} Ly6G⁺Ly6C⁻. ns, not significant, **p<0.01, ***p<0.001, ****p<0.0001, unpaired two-tailed Student's *t*-test.

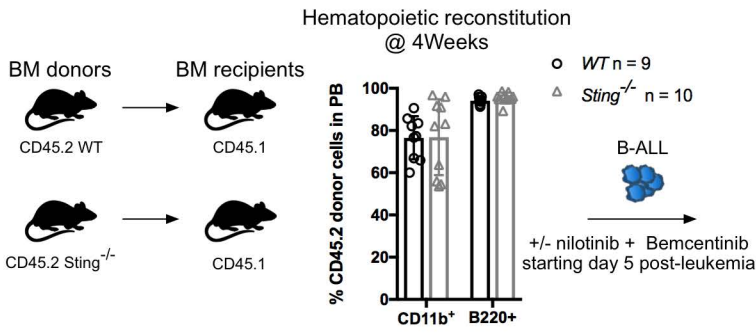
(D-E) Gating strategy and frequency of T regulatory cells (Foxp3⁺) within CD4⁺ T cells (GFP⁻CD45⁺CD3⁺CD4⁺) of mice used in (B-C). *p<0.05, ***p<0.001, ****p<0.0001, unpaired two-tailed Student's *t*-test.

(F-H) Gating strategy (F), frequencies of CD4 and CD8 T cells (G) as well as CD8 to CD4 T cell ratios (H) in the spleen and bone marrow of mice described in (B-C). The depicted percentages are out of non-leukemic GFP⁻CD45⁺ cells. *p<0.05, **p<0.01, ****p<0.0001, unpaired two-tailed Student's *t*-test.

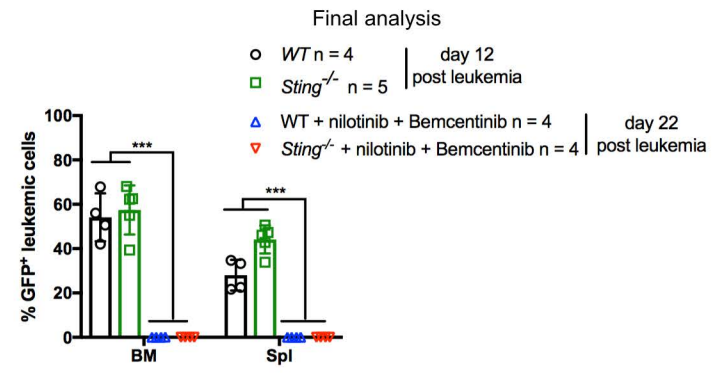
(I-J) Gating strategy and frequencies of NK cells (CD3⁻NK1.1⁺DX5⁺) in the non-leukemic GFP⁻CD45⁺ fraction of cells from the bone marrow and spleen of mice described in (B-C). ns, not significant, **p<0.01, unpaired two-tailed Student's *t*-test.

Figure S7

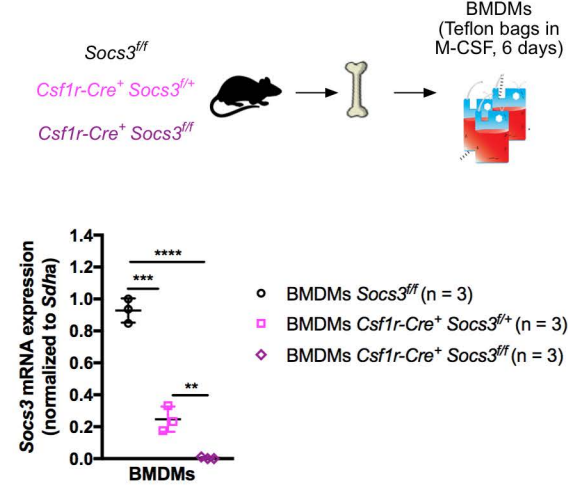
A



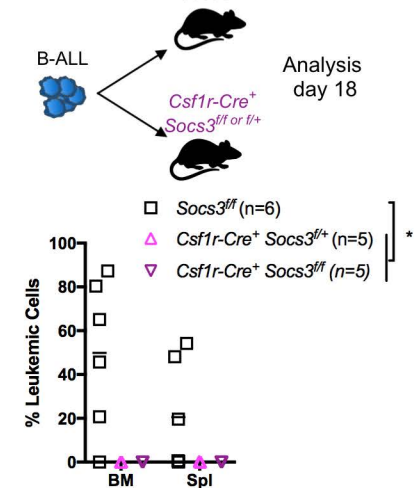
B



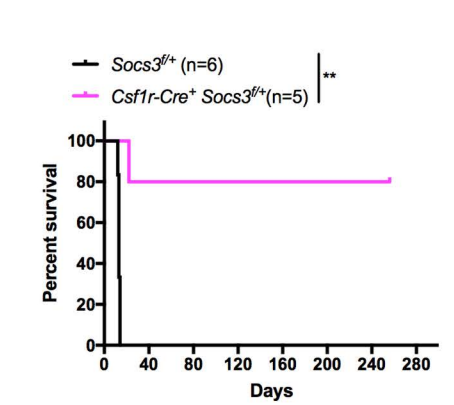
C



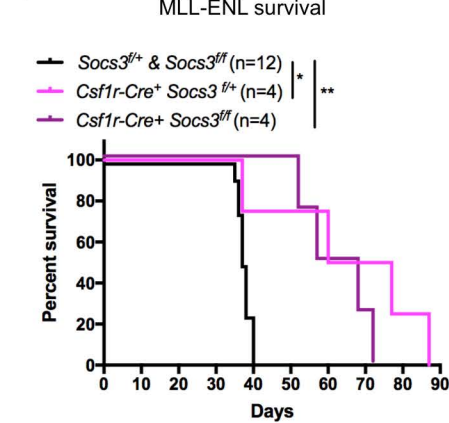
D



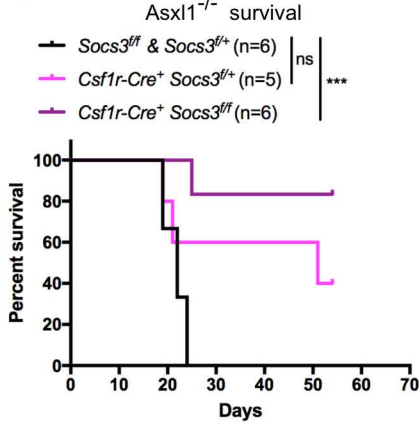
E



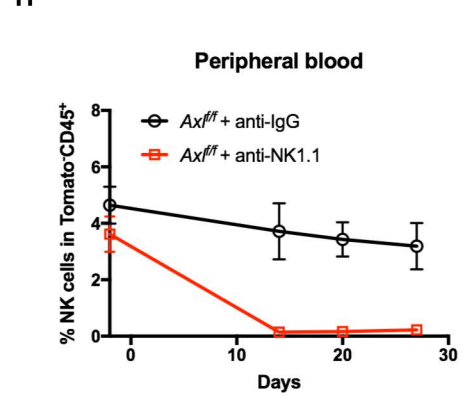
F



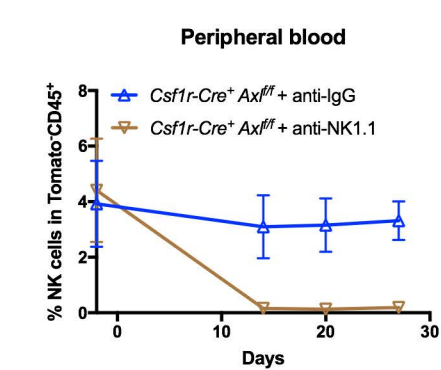
G



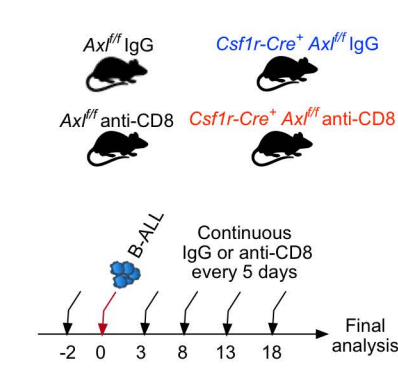
H



I



J



K

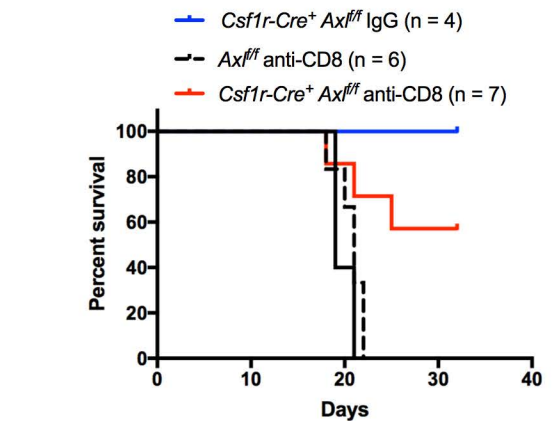


Figure S7. Downstream cellular and molecular mediators of the leukemia protective phenotype imposed by *Axl* deletion in macrophages.

(A) WT CD45.1 SJL mice were lethally irradiated and reconstituted with donor bone marrow cells from either CD45.2 WT (n = 9) or CD45.2 *Sting*^{-/-} (n = 10) mice. Percentage of CD45.2 donor cells depicts reconstitution at 4 weeks at which point the mice were challenged with 10³ B-ALL cells. 5 days later, mice from each genotype were randomized to receive either vehicle or treatment with nilotinib and Bemcentinib as indicated.

(B) Leukemic burden in spleen and bone marrow as evaluated by flow cytometry upon final analysis of both vehicle (day 12 post leukemia challenge) and treated (day 22 post leukemia challenge) cohorts. Both WT and *Sting*^{-/-} chimeras effectively cleared leukemia in response to the combination treatment. In (G), two mice (1 *Sting*^{-/-} and 1 WT) were not available for the final analysis due to accidental death unrelated to the experiment. ***p<0.001, unpaired two-tailed Student's *t*-test.

(C) *Socs3* expression by real time PCR in bone marrow-derived macrophages (BMDMs) from mice with the indicated genotypes. Each data point represents BMDMs from an independent mouse. **p<0.01, ***p<0.001, ****p<0.0001, unpaired two-tailed Student's *t*-test.

(D) Leukemic burden in the bone marrow and spleen of mice of the indicated genotypes 18 days post challenge with 10³ B-ALL cells. Each dot represents an independent mouse. *p<0.05, unpaired two-tailed Student's *t*-test.

(E-G) Kaplan Meier survival analysis of mice of the indicated genotypes challenged with either 10³ B-ALL cells (E), 10⁵ MLL-ENL AML cells (F) or 5.10⁵ *Asx1*^{-/-} AML cells (G). *p<0.05, **p<0.01, ***p<0.001, log-rank (Mantel-Cox) test.

(H-I) Frequencies of NK cells (CD45⁺GFP⁻CD3⁻NK1.1⁺DX5⁺) as evaluated by FACS in the experiment described in main Figure 4D.

(J-K) Kaplan-Meier survival analysis of mice of the indicated genotypes challenged with 10³ B-ALL cells and treated with either an anti-CD8 antibody or a Rat IgG2b isotype control every 5 days. Depletion was initiated 2 days before leukemia injection and maintained throughout the experiment. All deceased mice succumbed to *bona fide* GFP⁺ B220^{dim} B-ALL (data not shown).

Figure S8

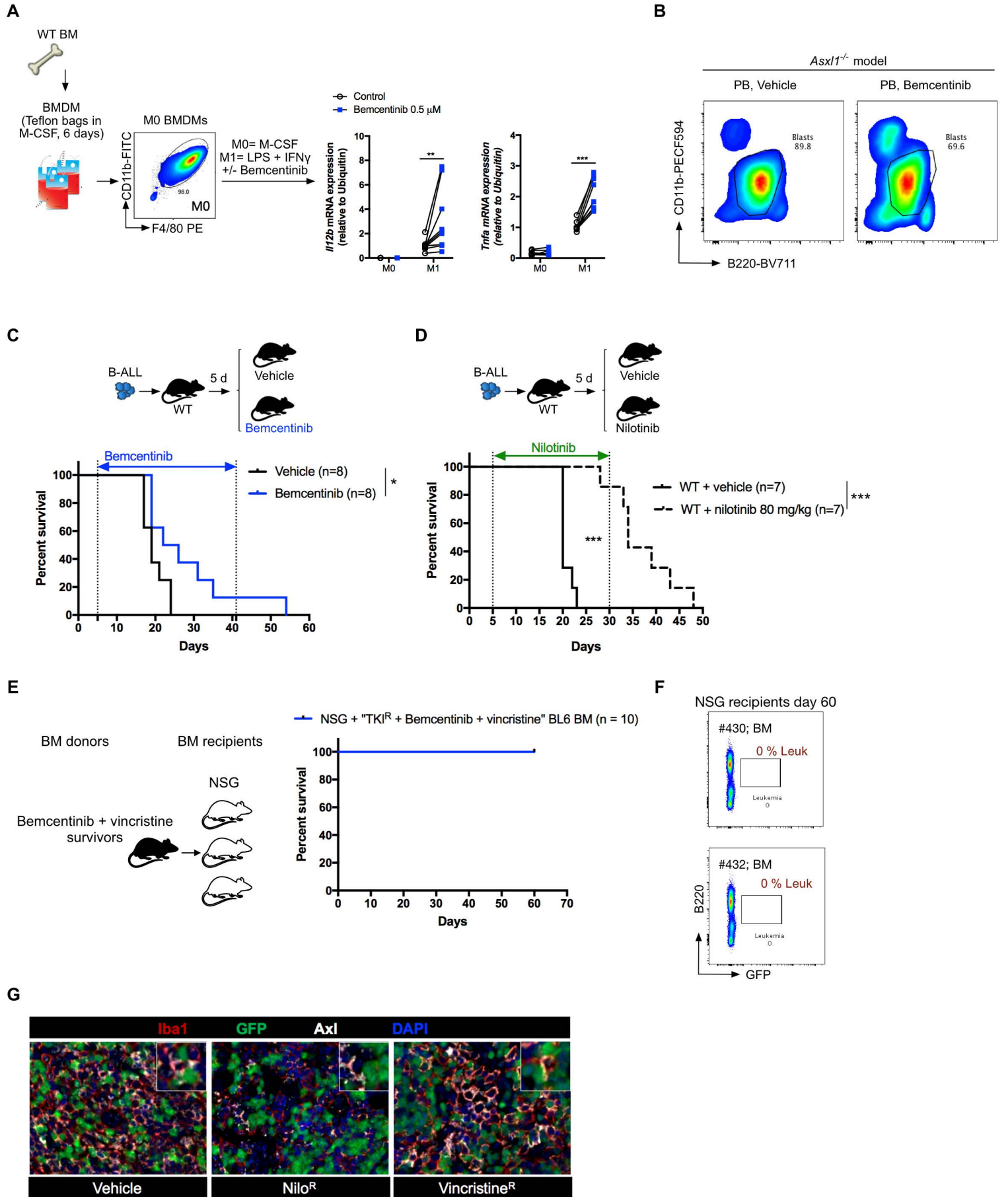


Figure S8. Therapeutic efficacy of a clinical grade AXL inhibitor, Bemcentinib.

(A) Bone marrow-derived macrophages from WT mice (BMDMs, n = 9 donors) were generated *in vitro* in the presence of M-CSF and either left untreated (M0) or stimulated, for 24h, with IFN γ and LPS to direct M1-like priming (M1), in the presence or absence of 0.5 μ M Bemcentinib. *Ii12b* and *Tnfa* expression was evaluated using real-time PCR. Data are mean \pm s.e.m. after normalization to a reference gene, *Ubc*. Data are pooled from 3 independent experiments. **p<0.01, ***p<0,001, Wilcoxon matched pairs signed rank test.

(B) Representative FACS data showing comparable phenotype in terminally ill mice from vehicle and BGB treated mice from Fig. 7A.

(C) Kaplan-Meier survival analysis of WT C57BL/6 mice challenged with 10³ B-ALL cells and randomized on day 5 to vehicle (n = 8) or Bemcentinib (n = 8). All mice succumbed to *bona fide* GFP⁺ B220⁺ leukemia (data not shown). *p<0.05, log-rank (Mantel–Cox) test.

(D) Kaplan Meier survival analysis of WT C57BL/6 mice transplanted with 10³ GFP⁺ B-ALL cells and randomized on day 5 to vehicle or nilotinib (80 mg/kg/day) treatment. ***p<0.001, log-rank (Mantel–Cox) test.

(E) Kaplan-Meier survival analysis of NSG mice transplanted with 10⁷ bone marrow cells isolated from long-term survivors challenged with TKI^R B-ALL and treated with “bemcentinib + vincristine” described in Fig. 7G.

(F) Representative FACS plots of bone marrow from two independent NSG mice from E, at final analysis on day 60.

(G) Representative images of multiplex immunohistochemistry staining for Axl, Iba1 and GFP in spleen sections from untreated or therapy resistant (nilotinib resistant = Nilo^R GFP⁺; vincristine resistant = Vincristine^R GFP⁺) B-ALL bearing mice. IBA1⁺ macrophages (Red), GFP⁺ blasts (Green), AXL (White), nuclei (Blue).

For all experiments, Treatments were initiated and stopped on the days indicated by dotted lines.

Sample ID	Diagnosis	Sex	Age	Used in
#10441	Ph+ B-ALL	M	36	Figure 1B
#13693	Ph+ B-ALL	M	30	Figure 1B
#686	B-ALL	M	20	Figure 1B
#3355	T-ALL	F	37	Figure S1B
#11209	T-ALL	M	23	Figure S1B
BSD#1	Healthy	M	42	Figure 1C
BSD#2	Healthy	M	37	Figure 1C
BSD#3	Healthy	F	46	Figure 1C
BSD#4	Healthy	M	32	Figure 1C
BSD#5	Healthy	M	73	Figure 1C
BSD#6	Healthy	F	52	Figure 1C
BSD#7	Healthy	M	35	Figure 1C
BSD#8	Healthy	M	58	Figure 1C
BSD#9	Healthy	F	48	Figure 1C
BSD#10	Healthy	M	24	Figure 1C
BSD#11	Healthy	F	60	Figure 1C
BSD#12	Healthy	F	53	Figure 1C
B-ALL#V	Ph+ B-ALL	ND	adult	Figure 1C
B-ALL#M	Ph+ B-ALL	ND	adult	Figure 1C
#0202	AML	M	81	Figure 1C
#0401	High risk MDS	F	84	Figure 1C

Table S1. Description of the human samples used in this study